The dark matter halo from hydrodynamic simulations

Nassim Bozorgnia

GRAPPA Institute
University of Amsterdam

Based on work done with F. Calore, M. Lovell, G. Bertone, and the EAGLE team
arXiv: 1601.04707

GRAPPA GRavitation AstroParticle Physics Amsterdam

UNIVERSITY OF AMSTERDAM

Outline

- Dark matter direct detection
- Hints for a signal versus constraints
- DM distribution from cosmological simulations
  - Identifying simulated Milky Way analogues
  - Local DM density
  - Local DM velocity distribution
- Analysis of direct detection data
- Summary

Outline

- Dark matter direct detection
- Hints for a signal versus constraints
- DM distribution from cosmological simulations
  - Identifying simulated Milky Way analogues
  - Local DM density
  - Local DM velocity distribution
- Analysis of direct detection data
- Summary

Dark matter halo

- Very little is known about the details of the dark matter (DM) halo in the local neighborhood.

Dark matter halo

- Very little is known about the details of the dark matter (DM) halo in the local neighborhood.
- This introduces significant uncertainty when interpreting data from direct detection experiments.

Dark matter halo

- Very little is known about the details of the dark matter (DM) halo in the local neighborhood.
- This introduces significant uncertainty when interpreting data from direct detection experiments.
- Usually the **Standard Halo Model (SHM)** is assumed: isothermal sphere with an isotropic Maxwell-Boltzmann velocity distribution.
  - local DM density: $\rho_\chi \sim 0.3$ GeV cm^{-3}
  - typical DM velocity: $\bar{v} \simeq 220$ km/s

Dark matter halo

- Very little is known about the details of the dark matter (DM) halo in the local neighborhood.
- This introduces significant uncertainty when interpreting data from direct detection experiments.
- Usually the **Standard Halo Model (SHM)** is assumed: isothermal sphere with an isotropic Maxwell-Boltzmann velocity distribution.
  - local DM density: $\rho_\chi \sim 0.3$ GeV cm^{-3}
  - typical DM velocity: $\bar{v} \simeq 220$ km/s
- Numerical simulations of galaxy formation predict dark matter velocity distributions which can deviate from a Maxwellian.

Dark matter direct detection

- Strong tension between hints for a signal and exclusion limits (for elastic spin-independent scattering):

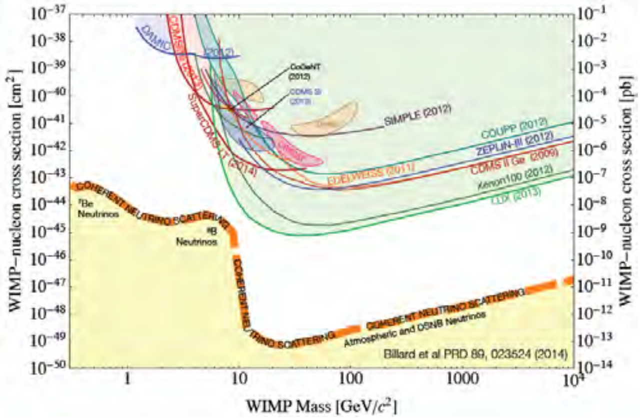

- Strong tension between hints for a signal and exclusion limits (for elastic spin-independent scattering):

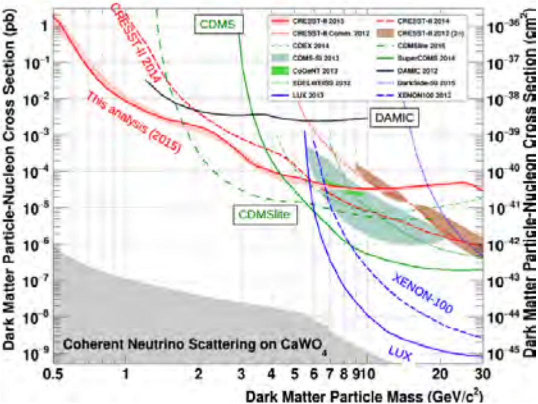

- Strong tension between hints for a signal and exclusion limits (for elastic spin-independent scattering):

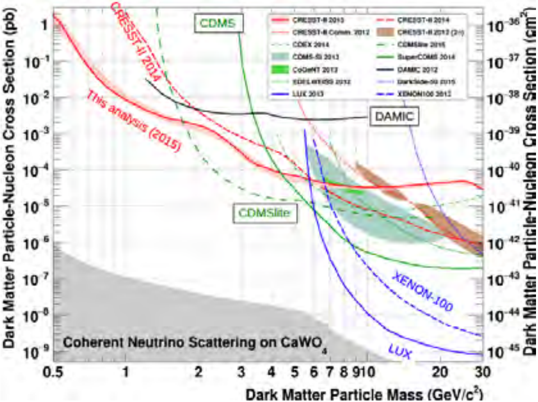

- These kinds of plots assume the Standard Halo Model and a specific DM-nucleus interaction.

Our aim

- Identify Milky Way-like galaxies from high resolution hydrodynamic simulations, by taking into account observational constraints on the Milky Way (MW).
- Extract the DM density and velocity distribution at the Solar position for the selected MW analogues.
- Analyze the data from direct detection experiments, using the local DM distributions of the selected haloes.

Dark matter direct detection

- Look for energy deposited in low-background detectors by the scattering of WIMPs in the dark halo of our galaxy.
- WIMP-nucleus collision:

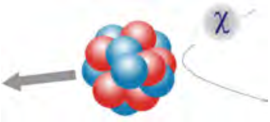

Dark matter direct detection

- Look for energy deposited in low-background detectors by the scattering of WIMPs in the dark halo of our galaxy.
- WIMP-nucleus collision:

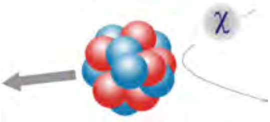

- Elastic recoil energy:

$$E_R = \frac{2\mu_{\chi A}^2 v^2}{m_A} \cos^2 \theta_{\rm lab}$$

$\theta_{\rm lab}$: angle of the nuclear recoil relative to the initial WIMP direction

Dark matter direct detection

- Look for energy deposited in low-background detectors by the scattering of WIMPs in the dark halo of our galaxy.
- WIMP-nucleus collision:

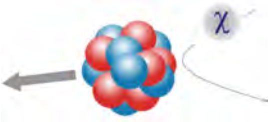

- Elastic recoil energy:

$$E_R = \frac{2\mu_{\chi A}^2 v^2}{m_A} \cos^2\theta_{\rm lab}$$

$\theta_{\rm lab}$: angle of the nuclear recoil relative to the initial WIMP direction

- Minimum WIMP speed required to produce a recoil energy E_R:

$$\boxed{v_m = \sqrt{\frac{m_A E_R}{2\mu_{\chi A}^2}}}$$

The differential event rate

- The differential event rate (event/keV/kg/day):

$$R(E_R, t) = \frac{\rho_\chi}{m_\chi} \frac{1}{m_A} \int_{v>v_m} d^3v \, \frac{d\sigma_A}{dE_R} \; v \; f_{\rm det}(\mathbf{v}, t)$$

The differential event rate

- The differential event rate (event/keV/kg/day):

$$R(E_R, t) = \frac{\rho_\chi}{m_\chi} \frac{1}{m_A} \int_{v>v_m} d^3v \frac{d\sigma_A}{dE_R} \; v \; f_{\rm det}(\mathbf{v}, t)$$

- For the standard spin-independent and spin-dependent scattering:

$$\frac{d\sigma_A}{dE_R} = \frac{m_A}{2\mu_{\chi A}^2 v^2} \sigma_0 F^2(E_R)$$

The differential event rate

- The differential event rate (event/keV/kg/day):

$$R(E_R, t) = \frac{\rho_\chi}{m_\chi} \frac{1}{m_A} \int_{v > v_m} d^3 v \frac{d\sigma_A}{dE_R} \; v \; f_{\rm det}(\mathbf{v}, t)$$

- For the standard spin-independent and spin-dependent scattering:

$$\frac{d\sigma_A}{dE_R} = \frac{m_A}{2\mu_{\chi A}^2 v^2} \sigma_0 F^2(E_R)$$

$$R(E_R, t) = \underbrace{\frac{\sigma_0 F^2(E_R)}{2 m_\chi \mu_{\chi A}^2}}_{\text{particle physics}} \; \underbrace{\rho_\chi \eta(v_m, t)}_{\text{astrophysics}}$$

where

$$\boxed{\eta(v_m, t) \equiv \int_{v > v_m} d^3 v \; \frac{f_{\rm det}(\mathbf{v}, t)}{v}} \qquad \text{halo integral}$$

Annual modulation

- Due to the motion of the Earth around the Sun, the velocity distribution in the Earth's frame changes in a year.

Max in June
Min in Dec

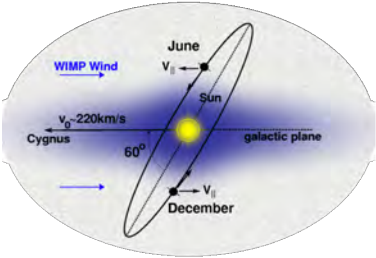

Annual modulation

- Due to the motion of the Earth around the Sun, the velocity distribution in the Earth's frame changes in a year.

Max in June
Min in Dec

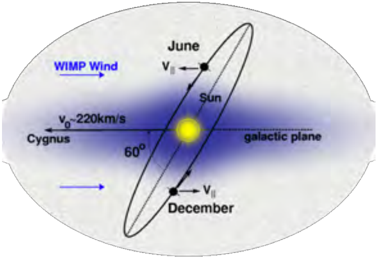

$$f_{\rm det}(\mathbf{v},t) = f_{\rm sun}(\mathbf{v}+\mathbf{v}_e(t)) = f_{\rm gal}(\mathbf{v}+\mathbf{v}_s+\mathbf{v}_e(t))$$

Sun's velocity wrt the Galaxy: $\mathbf{v}_s \approx (0, 220, 0) + (11, 12, 7)$ km/s

Earth's velocity: $v_e \approx 30$ km/s

Velocity distribution $f_{\text{gal}}(\mathbf{v})$?

- The velocity distribution depends on the halo model.

Velocity distribution $f_{\rm gal}(\mathbf{v})$?

- The velocity distribution depends on the halo model.
- In the SHM, a truncated Maxwellian velocity distribution is assumed

$$f_{\rm gal}(\mathbf{v}) \approx \begin{cases} N \exp(-\mathbf{v}^2/\bar{v}^2) & v < v_{\rm esc} \\ 0 & v \geq v_{\rm esc} \end{cases}$$

with $\bar{v} \simeq 220$ km/s, $v_{\rm esc} = 550$ km/s.

Velocity distribution $f_{\rm gal}(\mathbf{v})$?

- The velocity distribution depends on the halo model.
- In the SHM, a truncated Maxwellian velocity distribution is assumed

$$f_{\rm gal}(\mathbf{v}) \approx \begin{cases} N \exp(-\mathbf{v}^2/\bar{v}^2) & v < v_{\rm esc} \\ 0 & v \geq v_{\rm esc} \end{cases}$$

with $\bar{v} \simeq 220$ km/s, $v_{\rm esc} = 550$ km/s.

- DM distribution could be very different from Maxwellian:
  - Most likely both smooth and un-virialized (streams and debris flows) components.
  - the smooth component may not be Maxwellian.

Outline

- Dark matter direct detection
- Hints for a signal versus constraints
- DM distribution from cosmological simulations
  - Identifying simulated Milky Way analogues
  - Local DM density
  - Local DM velocity distribution
- Analysis of direct detection data
- Summary

Hints for a signal versus constraints

- Many direct dark matter experiments: **DAMA, XENON, CDMS, CoGeNT, CRESST, KIMS, LUX, SuperCDMS . . .**

Hints for a signal versus constraints

- Many direct dark matter experiments: **DAMA, XENON, CDMS, CoGeNT, CRESST, KIMS, LUX, SuperCDMS . . .**
- WIMPs interact with nuclei and produce:
  - **phonons, scintillation, or ionization**

Hints for a signal versus constraints

- Many direct dark matter experiments: **DAMA, XENON, CDMS, CoGeNT, CRESST, KIMS, LUX, SuperCDMS ...**
- WIMPs interact with nuclei and produce:
  - **phonons, scintillation, or ionization**
- We consider data from four experiments:

  Hints for a signal:

  - **DAMA:** scintillation (NaI)
  - **CDMS-Si:** ionization + phonons (Si)

  Null results:

  - **LUX:** scintillation + ionization (Xe)
  - **SuperCDMS:** ionization + phonons (Ge)

DAMA annual modulation signal

- NaI detectors; 9.3σ modulation signal; 1.33 ton yr (14 yrs)

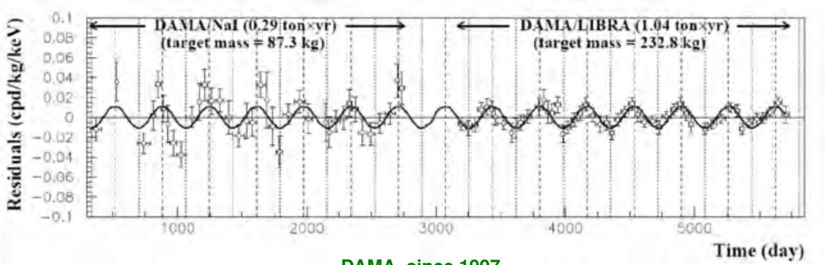

DAMA, since 1997

- Two possible WIMP masses: $m_\chi \sim 10$ GeV, $m_\chi \sim 80$ GeV

CDMS-Si excess of events

- 140.2 kg day in 8 Si detectors. Observed 3 events against expected background of 0.62 events.
- WIMP + background hypothesis favored over the known background estimate at $\sim 3\sigma$.

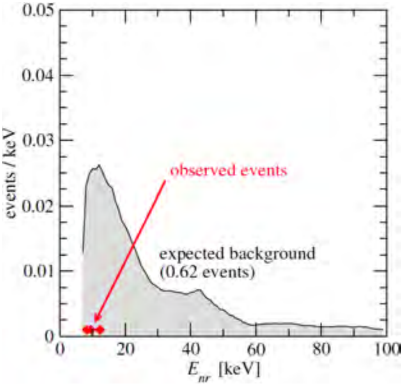

- Maximum likelihood at $m_\chi = 8.6$ GeV

Constraint from LUX and SuperCDMS

- Assuming the Standard Halo Model and spin-independent elastic scattering, strong tension between positive and negative results:

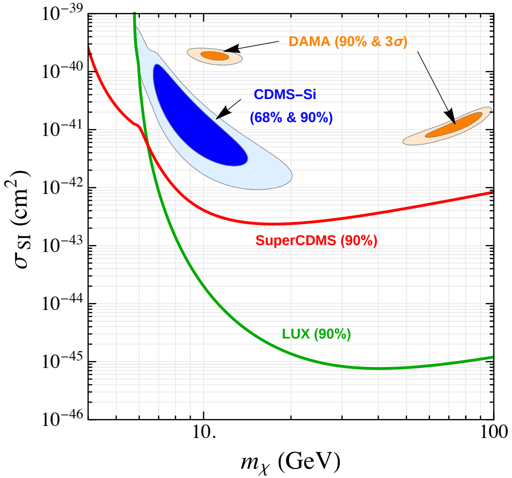

Outline

- Dark matter direct detection
- Hints for a signal versus constraints
- DM distribution from cosmological simulations
  - Identifying simulated Milky Way analogues
  - Local DM density
  - Local DM velocity distribution
- Analysis of direct detection data
- Summary

Hydrodynamic simulations

- We use the **EAGLE** and **APOSTLE** hydrodynamic simulations (**DM** + **baryons**).

Name	L (Mpc)	N	$m_{\rm g}$ ($\rm M_\odot$)	$m_{\rm dm}$ ($\rm M_\odot$)
EAGLE IR	100	6.8×10^9	1.81×10^6	9.70×10^6
EAGLE HR	25	8.5×10^8	2.26×10^5	1.21×10^6
APOSTLE IR	–	–	1.3×10^5	5.9×10^5

- **APOSTLE IR**: zoomed simulations of Local Group-analogue systems, comparable in resolution to **EAGLE HR**.

Hydrodynamic simulations

- We use the **EAGLE** and **APOSTLE** hydrodynamic simulations (**DM** + **baryons**).

Name	L (Mpc)	N	$m_{\rm g}$ ($\rm M_\odot$)	$m_{\rm dm}$ ($\rm M_\odot$)
EAGLE IR	100	6.8×10^9	1.81×10^6	9.70×10^6
EAGLE HR	25	8.5×10^8	2.26×10^5	1.21×10^6
APOSTLE IR	–	–	1.3×10^5	5.9×10^5

- **APOSTLE IR**: zoomed simulations of Local Group-analogue systems, comparable in resolution to **EAGLE HR**.
- These simulations are calibrated to reproduce the observed distribution of stellar masses and sizes of low-redshift galaxies.

Hydrodynamic simulations

- We use the **EAGLE** and **APOSTLE** hydrodynamic simulations (**DM** + **baryons**).

Name	L (Mpc)	N	$m_{\rm g}$ ($\rm M_\odot$)	$m_{\rm dm}$ ($\rm M_\odot$)
EAGLE IR	100	6.8×10^9	1.81×10^6	9.70×10^6
EAGLE HR	25	8.5×10^8	2.26×10^5	1.21×10^6
APOSTLE IR	–	–	1.3×10^5	5.9×10^5

- **APOSTLE IR**: zoomed simulations of Local Group-analogue systems, comparable in resolution to **EAGLE HR**.
- These simulations are calibrated to reproduce the observed distribution of stellar masses and sizes of low-redshift galaxies.
- Companion dark matter only (DMO) simulations were run assuming all the matter content is collisionless.

EAGLE simulations

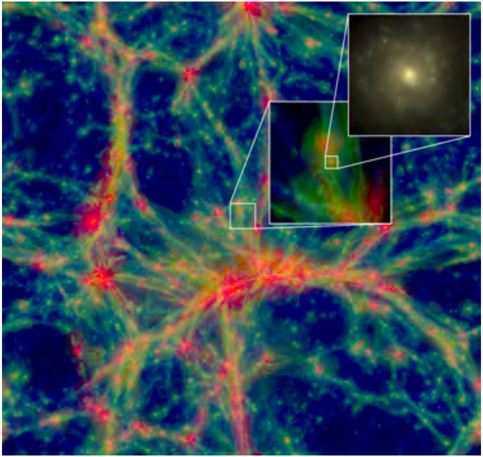

EAGLE project, 1407.7040

Intergalactic gas: blue $\Rightarrow$ green $\Rightarrow$ red with increasing temperature.

Milky Way analogues

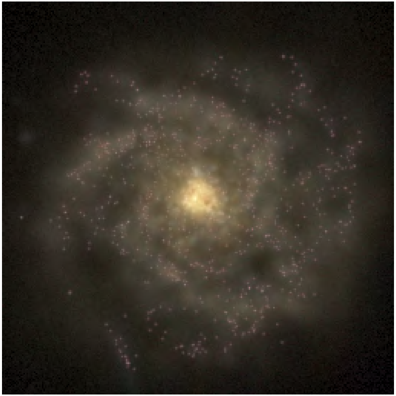

Identifying Milky Way analogues

- Usually a simulated halo is classified as *MW-like* if it satisfies the MW mass constraint, which has a large uncertainty. We demonstrate that the mass constraint is not enough to define a MW-like galaxy.

Identifying Milky Way analogues

- Usually a simulated halo is classified as *MW-like* if it satisfies the MW mass constraint, which has a large uncertainty. We demonstrate that the mass constraint is not enough to define a MW-like galaxy.
- Consider simulated haloes with $5 \times 10^{11} < M_{200}/\mathrm{M}_\odot < 2 \times 10^{13}$ and select the galaxies which most closely resemble the MW by the following criteria:
  - Rotation curve from simulation fits well the observed MW kinematical data from: [Iocco, Pato, Bertone, 1502.03821].
  - The total stellar mass of the simulated galaxies is within the 3σ observed MW range: $4.54 \times 10^{10} < M_*/\mathrm{M}_\odot < 8.32 \times 10^{10}$.

Observations vs. simulations

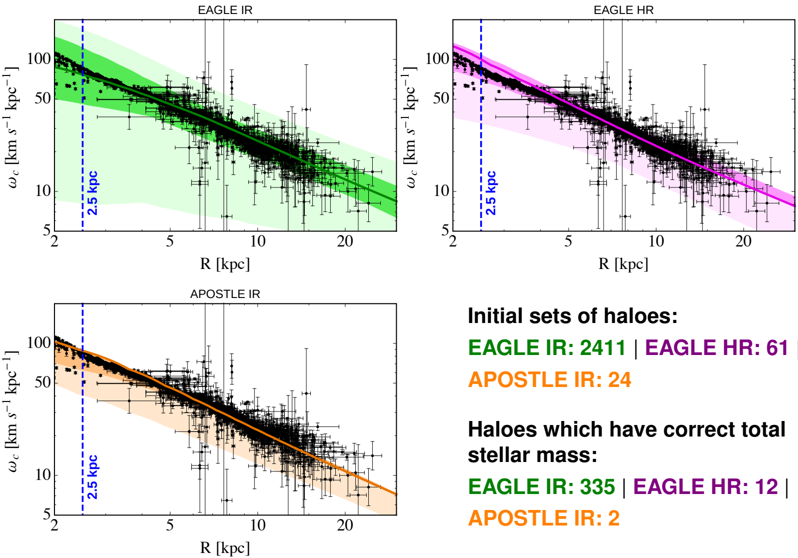

Initial sets of haloes:

EAGLE IR: 2411 | **EAGLE HR: 61** | **APOSTLE IR: 24**

Haloes which have correct total stellar mass:

EAGLE IR: 335 | **EAGLE HR: 12** | **APOSTLE IR: 2**

Observations vs. simulations

Goodness of fit to the observed data:

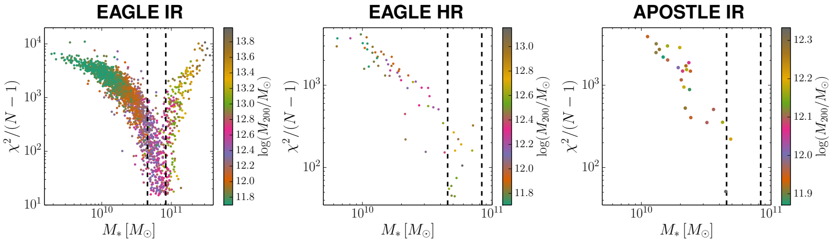

$N = 2687$ is the total number of observational data points used.

- Minimum of the reduced χ^2 occurs within the 3σ measured range of the MW total stellar mass. $\Rightarrow$ haloes with correct MW stellar mass have rotation curves which match well the observations.

Observations vs. simulations

Goodness of fit to the observed data:

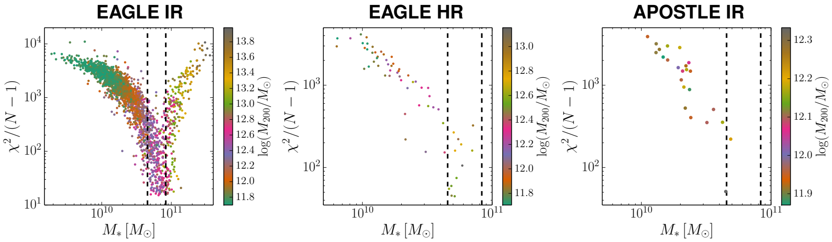

$N = 2687$ is the total number of observational data points used.

- Minimum of the reduced χ^2 occurs within the 3σ measured range of the MW total stellar mass. $\Rightarrow$ haloes with correct MW stellar mass have rotation curves which match well the observations.
- We focus only on the selected **EAGLE HR** and **APOSTLE IR** haloes due to higher resolution. $\Rightarrow$ total of **14** MW analogues.

Outline

- Dark matter direct detection
- Hints for a signal versus constraints
- DM distribution from cosmological simulations
  - Identifying simulated Milky Way analogues
  - Local DM density
  - Local DM velocity distribution
- Analysis of direct detection data
- Summary

Dark matter density profiles

- Spherically averaged DM density profiles derived from mass enclosed in a given spherical shell between R and $R + \delta R$:

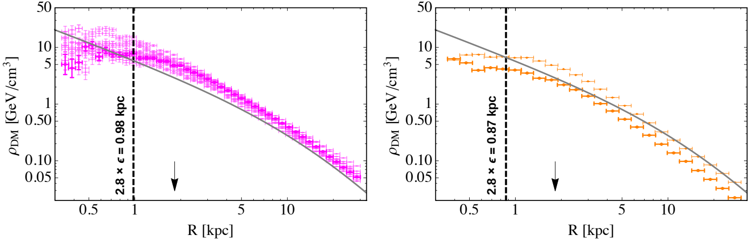

Dark matter density profiles

- Spherically averaged DM density profiles derived from mass enclosed in a given spherical shell between R and $R + \delta R$:

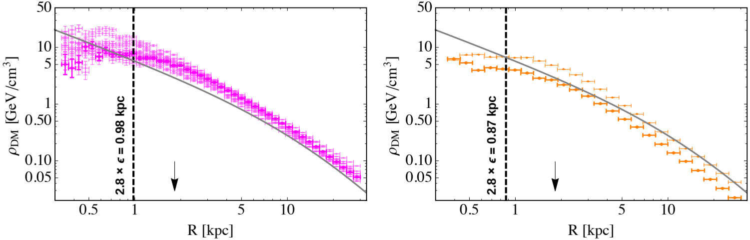

- In the inner 1.5 – 2 kpc: DM density shallower than NFW.
- Between 1.5 – 6/8 kpc: baryons lead to a steepening of the DM profile.

Local dark matter density

- Need the DM density at the position of the Sun.
- Consider a torus aligned with the stellar disc with $7 < R < 9$ kpc, and $-1 < z < 1$ kpc.

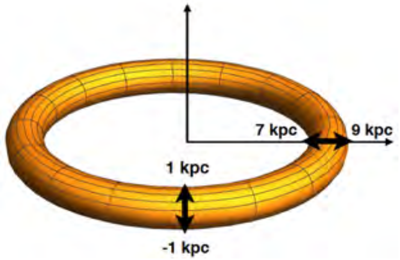

- **EAGLE HR**: local $\rho_{\rm DM} = 0.42 - 0.73$ GeV cm^{-3}.
- **APOSTLE IR**: local $\rho_{\rm DM} = 0.41 - 0.54$ GeV cm^{-3}.

Local dark matter density

Is there an enhancement of the local DM density in the **Galactic disc** compared to the **halo**?

Local dark matter density

Is there an enhancement of the local DM density in the **Galactic disc** compared to the **halo**?

- Compare the the average $\rho_{\rm DM}$ in the torus with the value in a spherical shell at $7 < R < 9$ kpc.

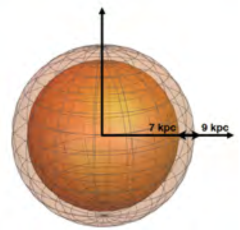

$\rho_{\rm DM}^{\rm torus}$ is larger than $\rho_{\rm DM}^{\rm shell}$ by:

2 – 27% for 10 haloes,
greater than 10% for 5 haloes, and
greater than 20% for only two haloes.

Local dark matter density

Is there an enhancement of the local DM density in the **Galactic disc** compared to the **halo**?

- Compare the the average $\rho_{\rm DM}$ in the torus with the value in a spherical shell at $7 < R < 9$ kpc.

  $\rho_{\rm DM}^{\rm torus}$ is larger than $\rho_{\rm DM}^{\rm shell}$ by:

  2 – 27% for 10 haloes,
  greater than 10% for 5 haloes, and
  greater than 20% for only two haloes.

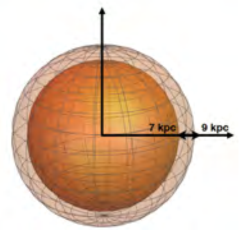

- The increase in the DM density in the disc could be due to the DM halo contraction as a result of dissipational baryonic processes.

Halo shapes

- To study the shape of the inner ($R < 8$ kpc) DM haloes, we calculate the inertia tensor of DM particles within 5 and 8 kpc.
  $\Rightarrow$ ellipsoid with three axes of length $a \geq b \geq c$.

Halo shapes

- To study the shape of the inner ($R < 8$ kpc) DM haloes, we calculate the inertia tensor of DM particles within 5 and 8 kpc. $\Rightarrow$ ellipsoid with three axes of length $a \geq b \geq c$.
- Calculate the sphericity: $s = c/a$.
  - $s = 1$: perfect sphere. $s < 1$: increasing deviation from sphericity.

Halo shapes

- To study the shape of the inner ($R < 8$ kpc) DM haloes, we calculate the inertia tensor of DM particles within 5 and 8 kpc. $\Rightarrow$ ellipsoid with three axes of length $a \geq b \geq c$.

- Calculate the sphericity: $s = c/a$.
  - $s = 1$: perfect sphere. $s < 1$: increasing deviation from sphericity.
  - At 5 kpc, $s = [0.85, 0.95]$. At 8 kpc, s lower by less than 10%.

Halo shapes

- To study the shape of the inner ($R < 8$ kpc) DM haloes, we calculate the inertia tensor of DM particles within 5 and 8 kpc. $\Rightarrow$ ellipsoid with three axes of length $a \geq b \geq c$.
- Calculate the sphericity: $s = c/a$.
  - $s = 1$: perfect sphere. $s < 1$: increasing deviation from sphericity.
  - At 5 kpc, $s = [0.85, 0.95]$. At 8 kpc, s lower by less than 10%.
  - Due to dissipational baryonic processes, DM sphericity systematically higher in the hydrodynamic simulations compared to DMO haloes in which $s = [0.75, 0.85]$.

Halo shapes

- Describe a deviation from sphericity by the triaxiality parameter:

$$T = \frac{a^2 - b^2}{a^2 - c^2}$$

Halo shapes

- Describe a deviation from sphericity by the triaxiality parameter:

$$T = \frac{a^2 - b^2}{a^2 - c^2}$$

- Oblate systems, $a \approx b \gg c \Rightarrow T \approx 0$.

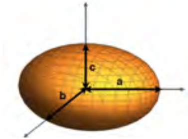

Halo shapes

- Describe a deviation from sphericity by the triaxiality parameter:

$$T = \frac{a^2 - b^2}{a^2 - c^2}$$

- Oblate systems, $a \approx b \gg c \Rightarrow T \approx 0$.

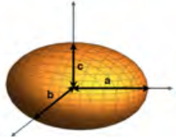

- Prolate systems, $a \gg b \approx c \Rightarrow T \approx 1$.

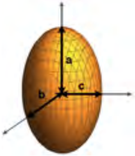

Halo shapes

- Describe a deviation from sphericity by the triaxiality parameter:

$$T = \frac{a^2 - b^2}{a^2 - c^2}$$

- Oblate systems, $a \approx b \gg c \Rightarrow T \approx 0$.

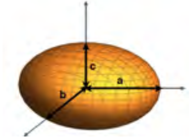

- Prolate systems, $a \gg b \approx c \Rightarrow T \approx 1$.

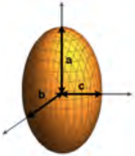

- In the hydro case, since inner haloes are very close to spherical, deviation towards either oblate or prolate is small. DMO counterparts have a preference for *prolate* inner haloes.

Outline

- Dark matter direct detection
- Hints for a signal versus constraints
- DM distribution from cosmological simulations
  - Identifying simulated Milky Way analogues
  - Local DM density
  - Local DM velocity distribution
- Analysis of direct detection data
- Summary

Local DM speed distributions

- DM speed distribution is related to the DM velocity distribution (in the Galactic rest frame):

$$f(|\mathbf{v}|) = v^2 \int d\Omega_{\mathbf{v}} \tilde{f}(\mathbf{v})$$

such that $\int dv \; f(|\mathbf{v}|) = 1$.

Local DM speed distributions

- DM speed distribution is related to the DM velocity distribution (in the Galactic rest frame):

$$f(|\mathbf{v}|) = v^2 \int d\Omega_{\mathbf{v}} \tilde{f}(\mathbf{v})$$

  such that $\int dv \; f(|\mathbf{v}|) = 1$.

- The torus contains 1800 – 3200 particles, depending on the halo.
- Due to limited resolution, we are not sensitive to the local variation of the DM velocity distribution within the torus. $\Rightarrow$ we take the average speed distribution of DM particles in the torus.

Local DM speed distributions

- DM speed distribution is related to the DM velocity distribution (in the Galactic rest frame):

$$f(|\mathbf{v}|) = v^2 \int d\Omega_{\mathbf{v}} \tilde{f}(\mathbf{v})$$

  such that $\int dv\ f(|\mathbf{v}|) = 1$.

- The torus contains 1800 – 3200 particles, depending on the halo.
- Due to limited resolution, we are not sensitive to the local variation of the DM velocity distribution within the torus. $\Rightarrow$ we take the average speed distribution of DM particles in the torus.
- Compare the DM speed distribution from simulations to:
  - SHM Maxwellian with $v_0 = 230$ km/s.
  - Maxwellian with free peak speed: $f(v) \propto v^2\ \exp[-(v/v_0)^2]$.

Local DM speed distributions

In the Galactic rest frame:

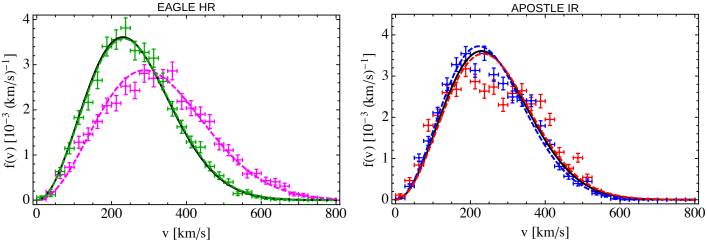

Local DM speed distributions

In the Galactic rest frame:

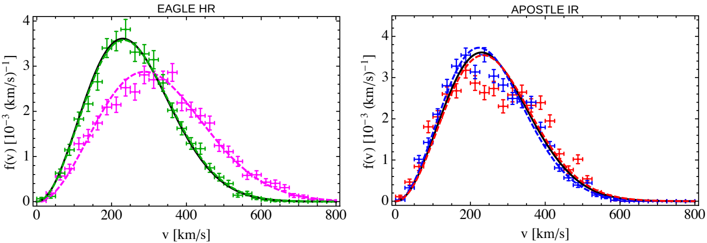

- Comparison to dark matter only (DMO) simulations:

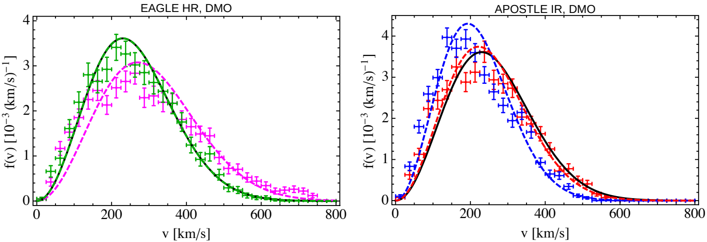

Local DM speed distribution

- Baryons deepen the gravitational potential of the Galaxy in the inner regions, resulting in more high velocity particles. $\Rightarrow$ The peak of the DM speed distribution is shifted to higher speeds when baryons are included in the simulations.

Local DM speed distribution

- Baryons deepen the gravitational potential of the Galaxy in the inner regions, resulting in more high velocity particles. $\Rightarrow$ The peak of the DM speed distribution is shifted to higher speeds when baryons are included in the simulations.
- The Maxwellian distribution with a free peak provides a better fit to haloes in the hydrodynamic simulations compared to their DMO counterparts.

Local DM speed distribution

- Baryons deepen the gravitational potential of the Galaxy in the inner regions, resulting in more high velocity particles. $\Rightarrow$ The peak of the DM speed distribution is shifted to higher speeds when baryons are included in the simulations.
- The Maxwellian distribution with a free peak provides a better fit to haloes in the hydrodynamic simulations compared to their DMO counterparts.
- The best fit peak speed of the Maxwellian distribution in the hydrodynamic simulations: 223 – 289 km/s.

Components of the velocity distribution

Distributions of radial, azimuthal, and vertical velocity components:

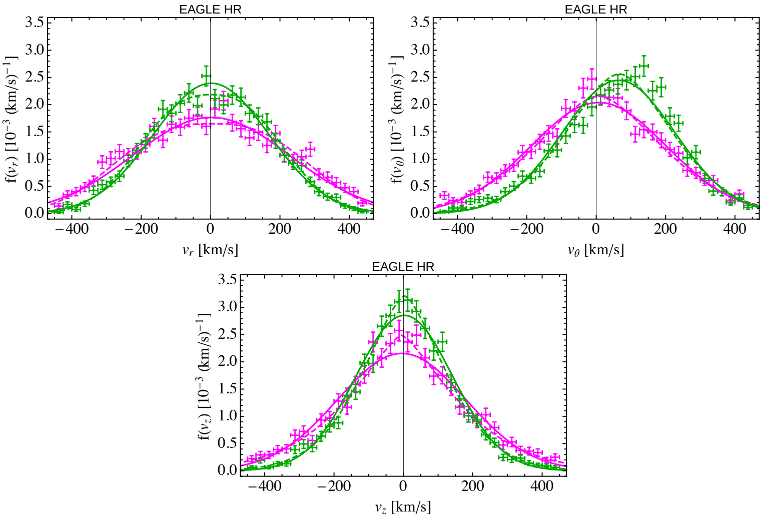

Components of the velocity distribution

Comparison to DMO simulations:

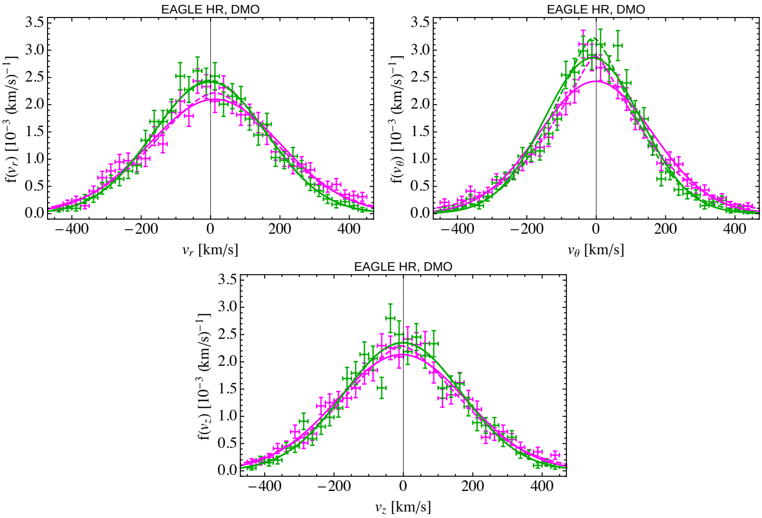

Components of the velocity distribution

- The three components of the DM velocity distribution are not similar. $\Rightarrow$ Clear velocity anisotropy at the Solar circle.
- The distributions of the **radial** and **vertical** velocity components are peaked around zero.

Components of the velocity distribution

- The three components of the DM velocity distribution are not similar. $\Rightarrow$ Clear velocity anisotropy at the Solar circle.
- The distributions of the **radial** and **vertical** velocity components are peaked around zero.
- Four haloes have a significant positive mean **azimuthal** speed ($\mu > 20$ km$/$s). The DMO counterparts of these haloes don't show evidence of rotation.

Components of the velocity distribution

- The three components of the DM velocity distribution are not similar. $\Rightarrow$ Clear velocity anisotropy at the Solar circle.
- The distributions of the **radial** and **vertical** velocity components are peaked around zero.
- Four haloes have a significant positive mean **azimuthal** speed ($\mu >$ 20 km/s). The DMO counterparts of these haloes don't show evidence of rotation.
- Is this pointing to the existence of a "dark disc"?

Dark disc

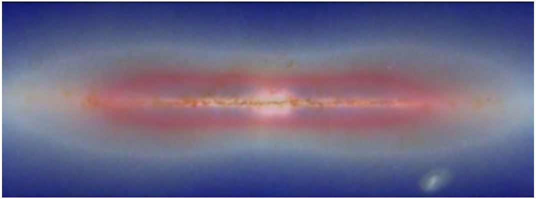

From images in 2MASS. Credit: J. Read & O. Agertz

- Dark disc forms when stars and gas in the Galactic disc drag merging satellites towards the Galactic plane. Tidal forces disrupt these satellites. $\Rightarrow$ their accreted material forms thick stellar and DM discs [Read, Lake, Agertz, Debattista, 0803.2714].

Dark disc

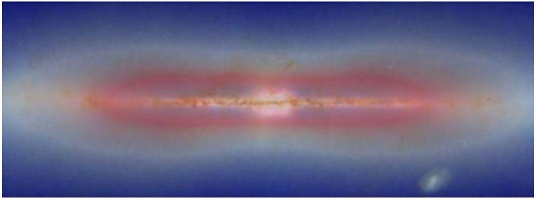

From images in 2MASS. Credit: J. Read & O. Agertz

- Dark disc forms when stars and gas in the Galactic disc drag merging satellites towards the Galactic plane. Tidal forces disrupt these satellites. ⇒ their accreted material forms thick stellar and DM discs [Read, Lake, Agertz, Debattista, 0803.2714].
- Implications for direct detection:
  - Density of the dark disc ⇒ Enhance direct detection event rates.
  - Lag velocity of the DM particles in the disc compared to the stellar particles ⇒ Shift in the phase of the annual modulation signal.

Dark disc in EAGLE and APOSTLE

- To check the existence of a dark disc in any of our MW analogues, we need to search for galaxies with a DM component rotating as fast as the stars.
- For each halo, we fit the **azimuthal velocity distribution** of the star and DM particles in the torus with a double Gaussian.

Dark disc in EAGLE and APOSTLE

- To check the existence of a dark disc in any of our MW analogues, we need to search for galaxies with a DM component rotating as fast as the stars.
- For each halo, we fit the **azimuthal velocity distribution** of the star and DM particles in the torus with a double Gaussian.
- Among the **four haloes** with significant positive mean azimuthal speed, **two haloes** have a rotating DM component in the disc with mean velocity comparable (within 50 km/s) to that of the stars.

Dark disc in EAGLE and APOSTLE

- To check the existence of a dark disc in any of our MW analogues, we need to search for galaxies with a DM component rotating as fast as the stars.
- For each halo, we fit the **azimuthal velocity distribution** of the star and DM particles in the torus with a double Gaussian.
- Among the **four haloes** with significant positive mean azimuthal speed, **two haloes** have a rotating DM component in the disc with mean velocity comparable (within 50 km/s) to that of the stars.
- Hint for the existence of a co-rotating dark disc in **2 out of 14** MW-like haloes. $\Rightarrow$ dark discs are relatively rare in our halo sample.

The halo integral

- The halo integral parametrizes the astrophysics dependence of the event rate,

$$\eta(v_m, t) \equiv \int_{v>v_m} d^3v \, \frac{f_{\rm det}(\mathbf{v}, t)}{v}, \quad R(E_R, t) = \frac{\rho_\chi \sigma_0 \, F^2(E_R)}{2 m_\chi \mu_{\chi A}^2} \, \eta(v_m, t)$$

- To compute the halo integral, we need the velocity distributions in the detector reference frame:

$$f_{\rm det}(\mathbf{v}, t) = f_{\rm gal}(\mathbf{v} + \mathbf{v}_s + \mathbf{v}_e(t))$$

The halo integral

- The halo integral parametrizes the astrophysics dependence of the event rate,

$$\eta(v_m, t) \equiv \int_{v>v_m} d^3v \, \frac{f_{\rm det}(\mathbf{v}, t)}{v}, \quad R(E_R, t) = \frac{\rho_\chi \sigma_0 \, F^2(E_R)}{2 m_\chi \mu_{\chi A}^2} \, \eta(v_m, t)$$

- To compute the halo integral, we need the velocity distributions in the detector reference frame:

$$f_{\rm det}(\mathbf{v}, t) = f_{\rm gal}(\mathbf{v} + \mathbf{v}_s + \mathbf{v}_e(t))$$

Sun's velocity wrt the Galaxy: $\mathbf{v}_s \approx (0, v_\star, 0) + (11.10, 12.24, 7.25)$ km/s

$v_\star$: local circular speed for the **simulated halo**.

The halo integral

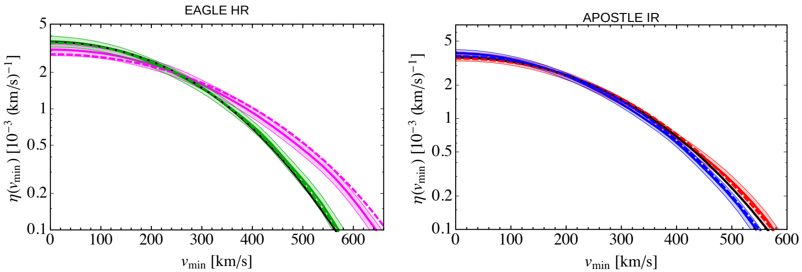

The halo integral

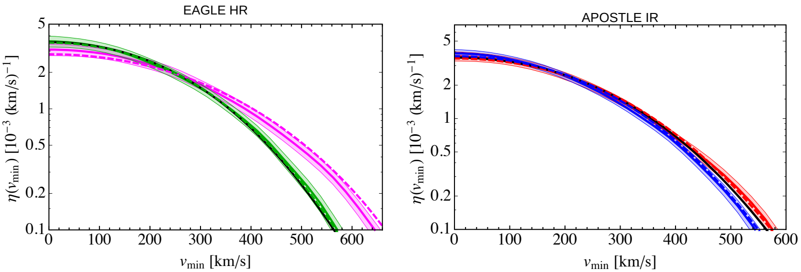

- Significant halo-to-halo scatter in the halo integrals.

The halo integral

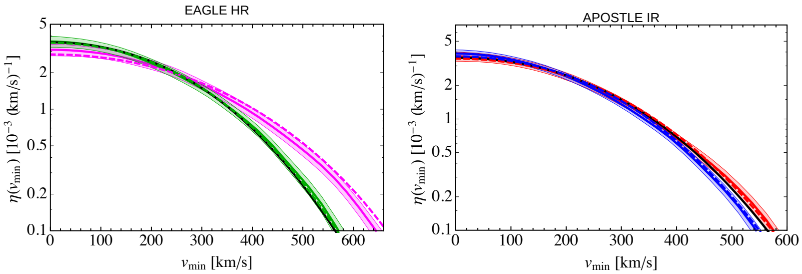

- Significant halo-to-halo scatter in the halo integrals.
- Halo integrals for the best fit Maxwellian velocity distribution (peak speed 223 – 289 km/s) fall within the 1σ uncertainty band of the halo integrals of the simulated haloes.

The halo integral

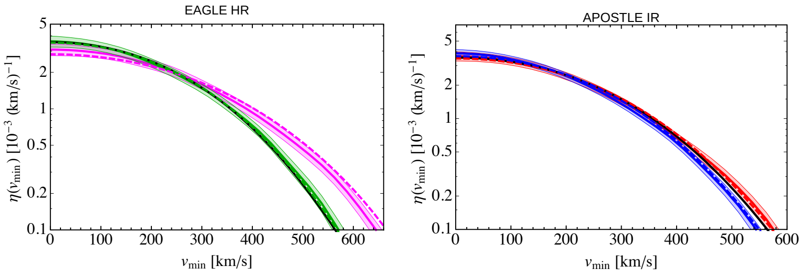

- Significant halo-to-halo scatter in the halo integrals.
- Halo integrals for the best fit Maxwellian velocity distribution (peak speed 223 – 289 km/s) fall within the 1σ uncertainty band of the halo integrals of the simulated haloes.
- Difference between simulated haloes and SHM Maxwellian due to the different peak speed of the DM velocity distribution of the simulated haloes compared to 230 km/s.

The halo integral

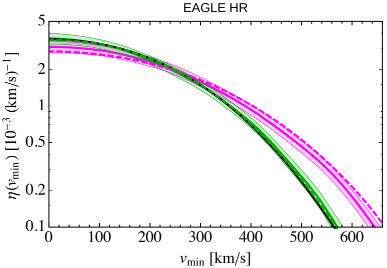

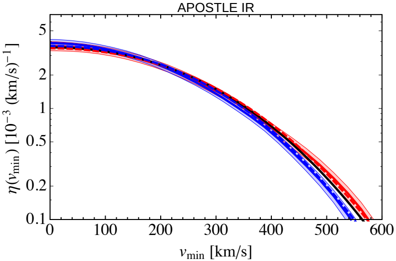

- Comparison to dark matter only (DMO) simulations:

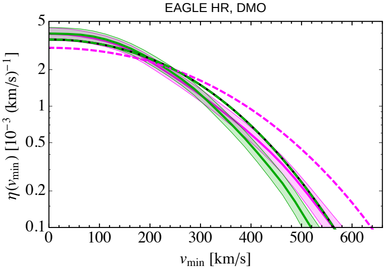

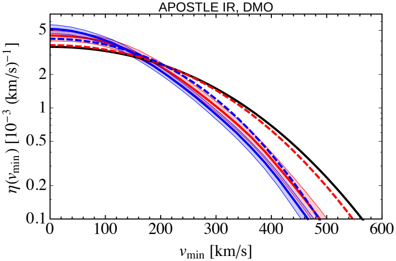

The halo integral

- Baryons affect the velocity distribution strongly at the Solar position, resulting in a shift of the tails of the halo integrals to higher velocities with respect to the DMO case.

The halo integral

- Baryons affect the velocity distribution strongly at the Solar position, resulting in a shift of the tails of the halo integrals to higher velocities with respect to the DMO case.
- Shape of speed distribution for DMO haloes not captured well by the Maxwellian with a free peak. There are large deficits at the peak, and an excess at low and very high velocities compared to the best fit Maxwellian speed distributions.

The halo integral

- Baryons affect the velocity distribution strongly at the Solar position, resulting in a shift of the tails of the halo integrals to higher velocities with respect to the DMO case.
- Shape of speed distribution for DMO haloes not captured well by the Maxwellian with a free peak. There are large deficits at the peak, and an excess at low and very high velocities compared to the best fit Maxwellian speed distributions.
- This results in quite different halo integrals of DMO haloes compared to their best fit Maxwellian halo integrals.

Outline

- Dark matter direct detection
- Hints for a signal versus constraints
- DM distribution from cosmological simulations
  - Identifying simulated Milky Way analogues
  - Local DM density
  - Local DM velocity distribution
- Analysis of direct detection data
- Summary

Implications for direct detection

- Assuming the SHM:

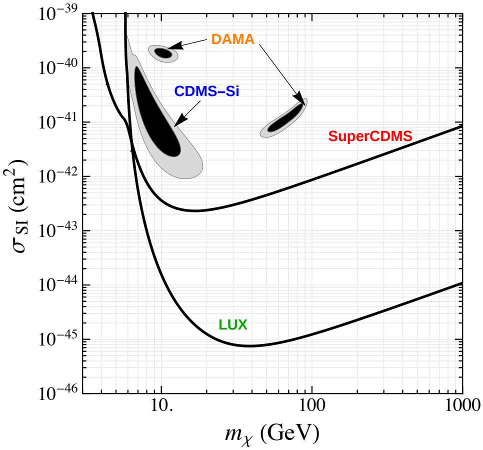

Implications for direct detection

- Comparing with simulated MW-like haloes in EAGLE HR (smallest ρ_{DM}):

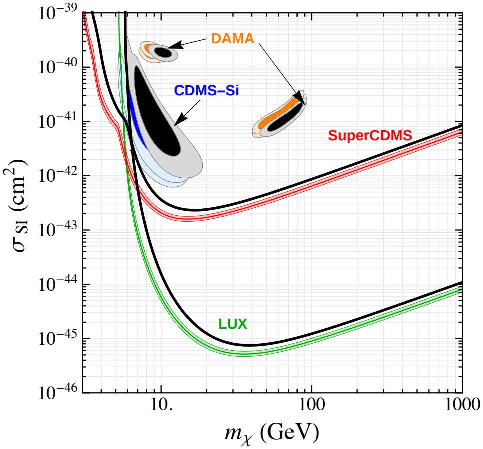

Implications for direct detection

- Comparing with simulated MW-like haloes in EAGLE HR (largest ρ_{DM}):

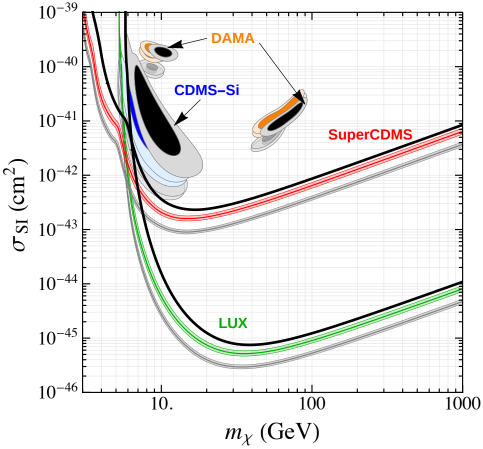

Implications for direct detection

- Comparing with simulated MW-like haloes in EAGLE HR (largest ρ_{DM}):

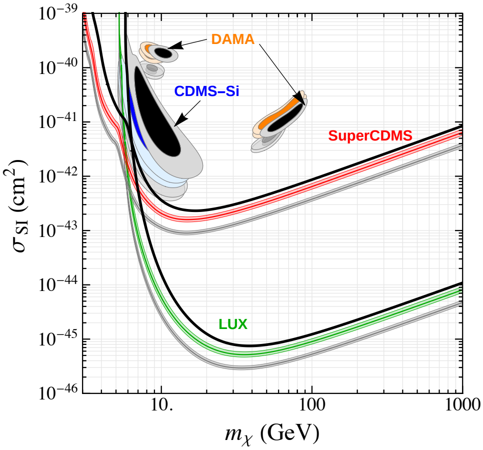

- Halo-to-halo uncertainty larger than the 1σ uncertainty from each halo.

Implications for direct detection

- Comparing with simulated MW-like haloes in EAGLE HR (largest ρ_{DM}):

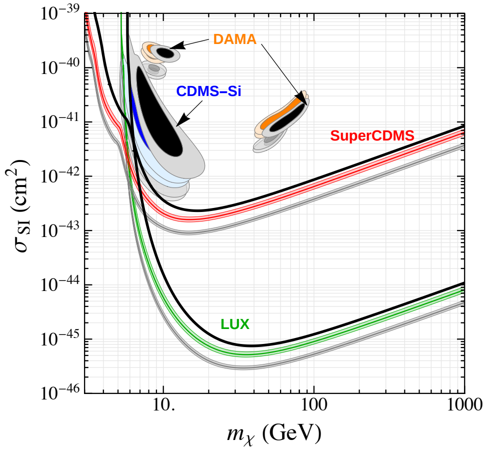

- Halo-to-halo uncertainty larger than the 1σ uncertainty from each halo.
- Overall difference with SHM mainly due to the different local DM density of the simulated haloes.

Effect of the velocity distribution

- Haloes in EAGLE HR with velocity distributions closest and farthest from SHM Maxwellian:

Fix local $\rho_{\rm DM} = 0.3$ GeV cm^{-3}

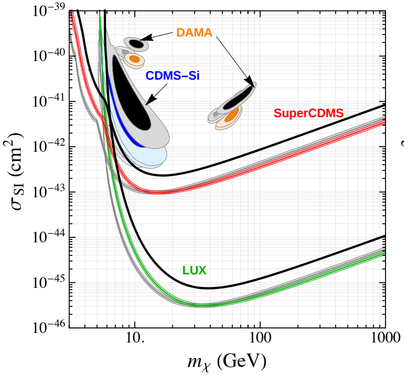

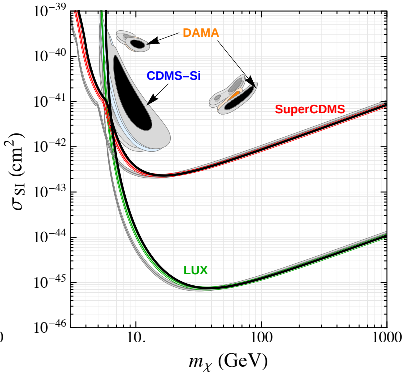

Effect of the velocity distribution

- Haloes in EAGLE HR with velocity distributions closest and farthest from SHM Maxwellian:

Fix local $\rho_{\rm DM} = 0.3$ GeV cm^{-3}

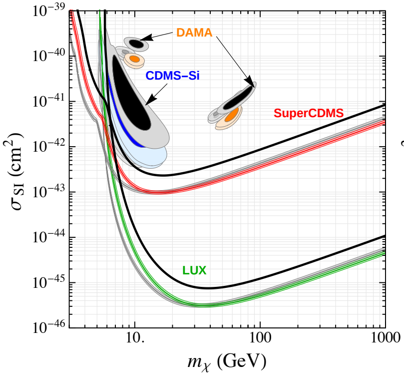

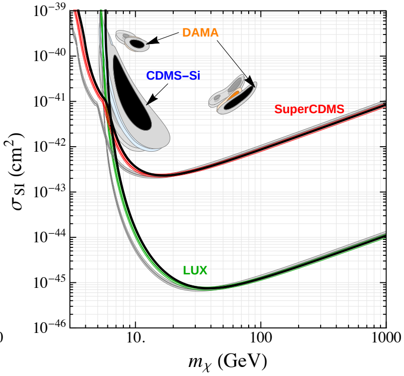

- Shift in the low WIMP mass region persists, where experiments probe the high velocity tail of the distribution.

Effect of the velocity distribution

- Haloes in APOSTLE IR:

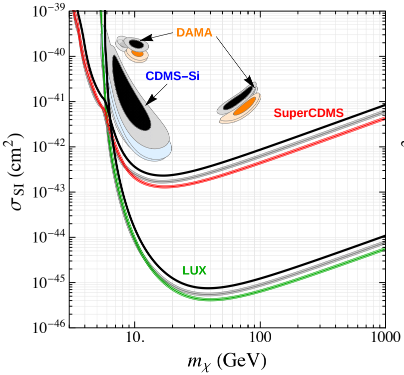

Fix local $\rho_{DM} = 0.3$ GeV cm^{-3}

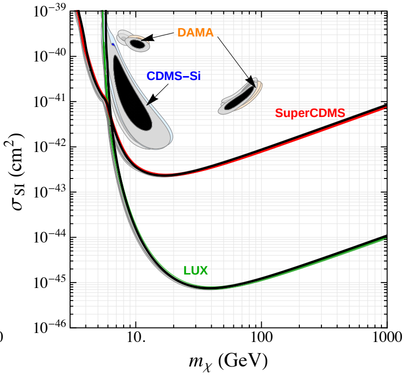

Effect of the velocity distribution

- Haloes in APOSTLE IR:

Fix local $\rho_{\rm DM} = 0.3$ GeV cm^{-3}

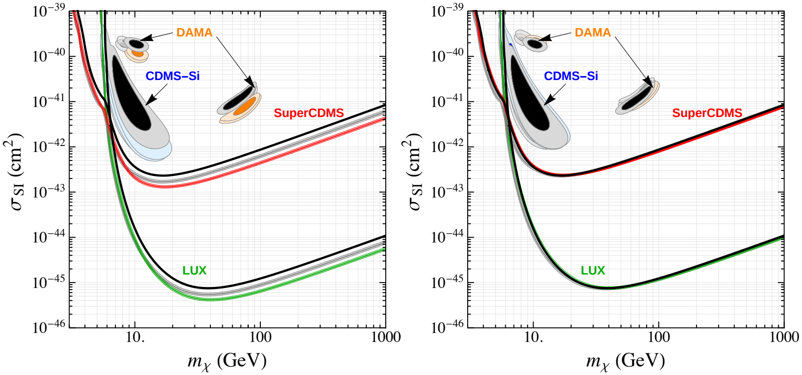

- Peak speed of the best fit Maxwellian is close to 230 km/s in APOSTLE IR haloes, so the effect of the velocity distribution is smaller.

Comparison with other recent works

- Kelso et al. 1601.04725, study two MW-like galaxies from the MaGICC simulations. Analogous to our findings, they also find that the best fit Maxwellian velocity distribution provides a good fit to the velocity distribution of each simulated halo.

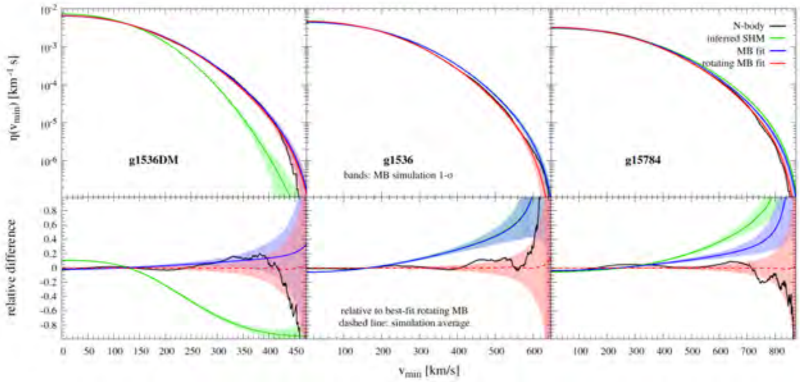

Comparison with other recent works

- Sloane et al. 1601.05402 study four MW-like galaxies with various merger histories.

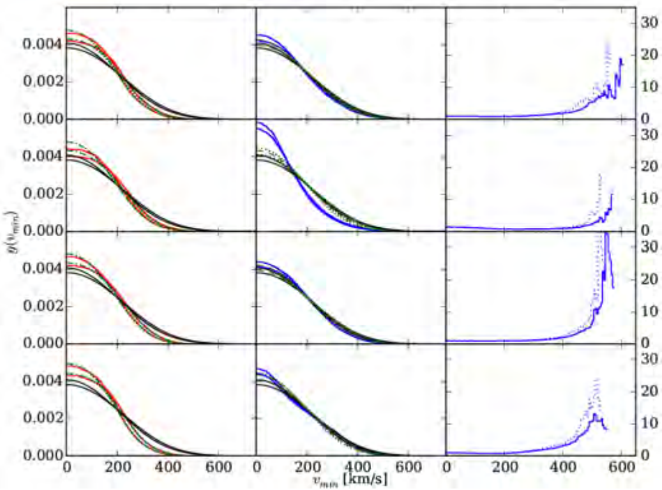

Comparison with other recent works

- Sloane et al. 1601.05402 study four MW-like galaxies with various merger histories.
- **Difference with our results:** they find a deficit of high speed DM particles in their simulations compared to the SHM.

Comparison with other recent works

- Sloane et al. 1601.05402 study four MW-like galaxies with various merger histories.
- **Difference with our results:** they find a deficit of high speed DM particles in their simulations compared to the SHM.
- However, the halo integrals obtained from their best fit Maxwellian velocity distributions show only small discrepancies at high speeds compared to those obtained from simulations.

Comparison with other recent works

- Sloane et al. 1601.05402 study four MW-like galaxies with various merger histories.
- **Difference with our results:** they find a deficit of high speed DM particles in their simulations compared to the SHM.
- However, the halo integrals obtained from their best fit Maxwellian velocity distributions show only small discrepancies at high speeds compared to those obtained from simulations.
- Difference between best fit peak speeds of the Maxwellian in our works likely due to the different stellar masses of our MW-like galaxies.

Comparison with other recent works

- The results of our work as well as Kelso et al. 1601.04725 and Sloane et al. 1601.05402 show that halo integrals and hence direct detection event rates obtained from a Maxwellian velocity distribution with a free peak speed are similar to those obtained directly from the simulated haloes.

Comparison with other recent works

- The results of our work as well as Kelso et al. 1601.04725 and Sloane et al. 1601.05402 show that halo integrals and hence direct detection event rates obtained from a Maxwellian velocity distribution with a free peak speed are similar to those obtained directly from the simulated haloes.
- A Maxwellian velocity distribution with a peak speed constrained by hydrodynamic simulations could be used by the community in the analysis of direct detection data.

Outline

- Dark matter direct detection
- Hints for a signal versus constraints
- DM distribution from cosmological simulations
  - Identifying simulated Milky Way analogues
  - Local DM density
  - Local DM velocity distribution
- Analysis of direct detection data
- Summary

Summary

- We identified simulated haloes which satisfy observational properties of the Milky Way, besides the uncertain mass constraint. Haloes are *MW-like* if:
  - good fit to observed MW rotation curve.
  - stellar mass in the 3σ observed MW stellar mass range.

Summary

- We identified simulated haloes which satisfy observational properties of the Milky Way, besides the uncertain mass constraint. Haloes are *MW-like* if:
  - good fit to observed MW rotation curve.
  - stellar mass in the 3σ observed MW stellar mass range.

- The local DM density: $\rho_{\rm DM} = 0.41 - 0.73$ GeV cm^{-3}. $\Rightarrow$ overall shift of the allowed regions and exclusion limits for all masses.

Summary

- We identified simulated haloes which satisfy observational properties of the Milky Way, besides the uncertain mass constraint. Haloes are *MW-like* if:
  - good fit to observed MW rotation curve.
  - stellar mass in the 3σ observed MW stellar mass range.
- The local DM density: $\rho_{\rm DM} = 0.41 - 0.73$ GeV cm^{-3}. $\Rightarrow$ overall shift of the allowed regions and exclusion limits for all masses.
- Halo integrals of MW analogues match well those obtained from best fit Maxwellian velocity distribution (with mean speed 223 – 289 km/s). $\Rightarrow$ shift of allowed regions and exclusion limits by a few GeV at low DM masses compared to SHM.

Summary

- We identified simulated haloes which satisfy observational properties of the Milky Way, besides the uncertain mass constraint. Haloes are *MW-like* if:
  - good fit to observed MW rotation curve.
  - stellar mass in the 3σ observed MW stellar mass range.
- The local DM density: $\rho_{\rm DM} = 0.41 - 0.73$ GeV cm^{-3}. $\Rightarrow$ overall shift of the allowed regions and exclusion limits for all masses.
- Halo integrals of MW analogues match well those obtained from best fit Maxwellian velocity distribution (with mean speed 223 – 289 km$/$s). $\Rightarrow$ shift of allowed regions and exclusion limits by a few GeV at low DM masses compared to SHM.
- Shift in the allowed regions and exclusion limits occurs in the same direction. $\Rightarrow$ compatibility between different experiments is not improved.

Additional slides

Selection criteria

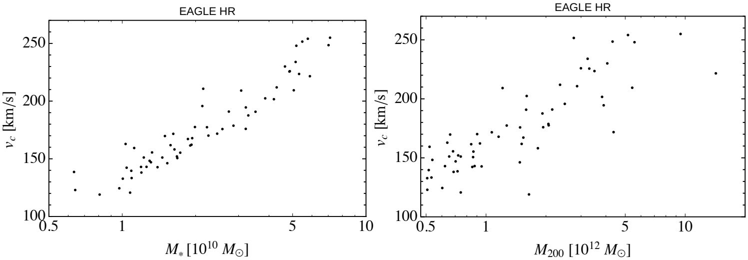

- $M_\star$ strongly correlated with v_c at 8 kpc, while the correlation of M_{200} with v_c is weaker.
- $M_\star(R < 8\ \mathrm{kpc}) = (0.5 - 0.9)M_\star$.
- $M_{\mathrm{tot}}(R < 8\ \mathrm{kpc}) = (0.01 - 0.1)M_{200}$.
- Over the small halo mass range probed, little correlation between $M_{\mathrm{DM}}(R < 8\ \mathrm{kpc})$ and M_{200}.

Velocity distribution azimuthal components

DM and stellar velocity distributions:

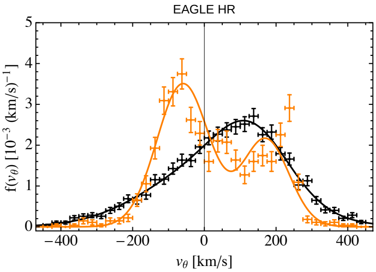

- Fit with a double Gaussian. Difference in the mean speed of second Gaussian between DM and stars is 35 km/s in the left, and 7 km/s in the right panel.
- Fraction of second Gaussian is 32% in the left panel and 43% in the right panel.